IUST
Iran University of Science and Technology

Iranian Journal of Electrical and Electronic Engineering

Journal Homepage: ijeee.iust.ac.ir

Mitigating the Effects of Rotary Transformer Leakage Flux on Brushless Synchro Accuracy

Mohammad Ali Razavi *, Farid Tootoonchian**(C.A.) and Zahra Nasiri-Gheidari*

Abstract: Synchros are electromagnetic sensors utilized to determine the angular position of a rotating shaft. This paper examines the impact of leakage flux from the Rotary Transformer (RT) on the induced voltages and the position detection accuracy of the Wound-Rotor (WR) synchro. Various methods are proposed to mitigate the negative effects of leakage flux from the RT. The leakage flux paths, which couple with the signal winding, are identified. Based on this analysis, the optimal distance between the sensor and the RT is calculated to minimize the adverse effects of leakage flux on the synchro's accuracy. Additionally, the RT structure is modified to reduce the leakage flux. Another effective approach involves the use of Electromagnetic Interference (EMI) shielding. In this context, a shield frame is designed for the RT, and the impact of different shield materials on reducing leakage flux is investigated. The results show that a copper-based shield significantly reduces the adverse effects of leakage flux and improves the sensor's accuracy. To evaluate the effectiveness of the proposed methods, they are assessed through 3-D Time-Stepping Finite Element Analysis (3-D TSFEA) and experimental measurements on a prototype sensor. The experimental results show close agreement with the 3-D TSFEA, confirming the accuracy of the findings.

Keywords: Brushless Synchro, Electromagnetic Interference (EMI) Shielding, Leakage Flux, Position Sensors, Rotary Transformer (RT), Time-Stepping Finite Element Analysis (TSFEA).

1 Introduction

POSITION sensors are widely employed in a variety of industrial applications today, such as in inverter-driven electrical machines with closed-loop control systems [1], robotic systems [2], transportation [3], and electric vehicles (EVs). Inverter-driven permanent magnet (PM) motors, known for their high power density and low torque ripple, are extensively used in EVs. The performance of these machines is strongly influenced by the motion control system, particularly the position sensor. To ensure optimal functionality, it is crucial to precisely determine the rotating shaft's position [4]. While many sensorless position estimation techniques are available, the inherent limitations of these methods in certain scenarios have led to the use of position sensors [5]. Sensors utilizing different technologies are available, with Hall-effect sensors, optical encoders, and selsyns being the most common types [1]. Among these, Hall-effect sensors are cost-effective but typically offer lower accuracy compared to other sensor types [6]. Optical encoders, though highly accurate and reasonably priced, have fragile physical structures, making them unsuitable for industrial environments subject to pollution, vibration, and wide temperature fluctuations [7]. In such cases, selsyns are preferred [8], as they are immune to environmental factors like humidity, dust, and oil [9].

A selsyn operates as a no-load synchronous generator, with its excitation winding powered by a high-frequency sinusoidal signal rather than a DC supply. Two-phase selsyns are referred to as resolvers, while three-phase ones are known as synchros [10]. Synchros, with their three-phase configurations, are more robust than

Iranian Journal of Electrical & Electronic Engineering, 2026.
Paper first received 22 Feb. 2025 and accepted 18 Aug. 225.
* The authors are with the Department of Electrical Engineering, Sharif University of Technology, Tehran, Iran.
E-mails: razavi.sma@ee.sharif.edu, znasiri@sharif.edu.
** The author is with the Department of Electrical Engineering, Iran University of Science and Technology, Tehran, Iran.
E-mail: tootoonchian@iust.ac.ir
Corresponding Author: Farid Tootoonchian.

resolvers, making them the ideal choice for applications demanding high reliability. However, the literature on resolvers is far more extensive than that on synchros. Research on resolvers includes new configurations and design improvements [11], [12], [13], [14], analytical models [15], [16], [17], performance assessments in both healthy and faulty conditions [18], [19], fault detection via resolver signals [20], fault-tolerant designs [21], [22], and new winding proposals [23], [24]. Due to the fine copper wire used in resolver windings, short-circuit or open-circuit faults are more likely to occur. If an open-circuit fault affects the two output windings, the sensor will fail [10]. However, an open-circuit fault in a single phase of the signal windings can be tolerated at the cost of decreased accuracy [22]. Therefore, for applications where sensor reliability is paramount, a three-phase selsyn, or synchro, is the most dependable choice. In terms of output wiring, synchros feature a three-wire output, while resolvers have four wires. For applications like EVs, where wiring volume is a critical factor, synchros are a more suitable option compared to resolvers. Conventional synchros have a Wound-Rotor (WR) connected to an AC voltage source via slip rings and brushes, and these are referred to as brushed synchros. The primary drawbacks of brushed synchros include voltage drop across the brushes, noise interference, reduced accuracy, and the need for frequent maintenance. To address these challenges, brushless technologies are employed [25]. To eliminate the maintenance costs of brushed synchros, the brushes have been removed, and a Rotary Transformer (RT) has been used in their place. The primary winding of the RT is fed with a high-frequency voltage source and is housed in a ferromagnetic core coupled to the stator of the synchro. The secondary winding, located within the RT's secondary core, is connected to the synchro's rotor. The voltage induced in the secondary winding provides power to the rotor's excitation winding, eliminating the need for brushes [26]. Since the RT and rotor are not physically connected, the lifespan of the RT is entirely dependent on the durability of the bearings [10]. The major benefits of WR synchros with RT include high tolerance to mechanical faults, exceptional positional accuracy [27], and silent operation. However, incorporating an RT into WR synchros presents challenges, such as increased sensor length, leakage flux interactions between the RT and synchro windings, and phase shift errors arising from the non-ideal nature of the RT's windings [28]. A potential solution to these challenges is removing the RT from the synchro's design. For example, [29] introduces a novel brushless synchro configuration, where the primary and secondary windings are placed on the stator, and the rotor consists of a ferromagnetic core with no copper windings. While this design eliminates the need for an RT, the accuracy and size of the sensor fall short of the required standards for a position sensor. A variable reluctance (VR) type of synchro, presented in [30], features a rotor without windings, with the excitation and signal windings placed on the stator. VR synchros offer benefits such as a more compact design due to the absence of an RT and simpler construction [30]. However, their position accuracy is highly sensitive to the precision of their installation on the electrical machine. Errors such as eccentricity and run-out can distort their output position significantly [20]. Other research focuses on improving WR synchro accuracy and simplifying winding designs. In [10], a method for distributing signal windings based on Tingley's scheme is proposed, along with an analysis of how different winding configurations affect WR synchro accuracy. Additionally, [31] proposes a novel winding method using matrix computations to simplify the conversion of synchro's three-phase outputs into resolver format without requiring Scott-T transformers. Both [10] and [31] avoid integrating the RT and synchro into a single frame, instead using separate frames for the RT and synchro to minimize the coupling of RT leakage flux with the synchro's windings.

Finally, to the best of the authors' knowledge, while the RT's leakage flux significantly affects WR sensor accuracy, only [32] provides an assessment of this issue. However, the compensation methods proposed in [32] do not fully resolve the problem. Therefore, this paper investigates the impact of RT leakage flux on synchro position error using 3-D finite element analysis and proposes several compensation techniques to mitigate its negative effects. In this regard, the optimal distance between the synchro and RT is determined to minimize the influence of leakage flux. Additionally, the RT structure is modified to reduce leakage flux, and an Electromagnetic Interference (EMI) shielding frame is designed and implemented to improve WR synchro accuracy. Experimental measurements are conducted to validate the effectiveness of the proposed methods.

2 Studied WR-Synchro Structure

The analyzed sensor is a brushless, cylindrical WR synchro equipped with an RT. As shown in Fig. 1, the stator features a 12-slot, three-phase, 2-pole configuration with concentrated windings. The rotor, consisting of 20 slots, has a single-phase, 2-pole concentrated winding. The number of turns for the excitation and signal windings on the i^{th} tooth can be calculated as [10]:

$$N_{sig-A,i} = N_{s,max}\, cos\, P_w[\frac{2\pi}{Z}(i-1)] \quad (1)$$

$$N_{sig-B,i} = N_{s,max}\, cos\, P_w[\frac{2\pi}{Z}(i-1)+120°] \quad (2)$$

$$N_{sig-C,i} = N_{s,max}\, cos\, P_w[\frac{2\pi}{Z}(i-1)-120°] \quad (3)$$

$$N_{exc,i} = N_{e,max}\, cos\, P_w[\frac{2\pi}{Z}(i-1)] \quad (4)$$

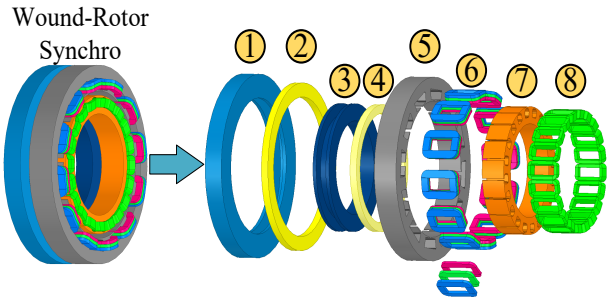

1. Primary Core of RT
2. Primary Coil of RT
3. Secondary Core of RT
4. Secondary Coil of RT
5. Stator Core
6. Signal Winding
7. Rotor Core
8. Excitation Winding

Fig 1. Schematic of the studied WR synchro with on-tooth winding.

where $N_{s,max}$ denotes the maximum number of turns for the signal winding, $N_{e,max}$ is the maximum number of turns for the excitation winding, Z represents the number of teeth, and P_w indicates the number of pole pairs. The geometrical dimensions and excitation specifications of the studied synchro are provided in Table I.

3 The Influence of RT

Given the configuration of the examined synchro, a 2-D analysis is not feasible. Therefore, to evaluate its performance, 3-D Time-Stepping Finite Element Analysis (TSFEA) is employed as a reliable method, using the ANSYS Electromagnetics Suite 2022 environment. However, the accuracy of the TSFEA depends on both the mesh resolution and the simulation time step. Finer meshes and shorter time steps lead to more accurate results, but come at the cost of increased computational demand. As a result, a balance must be struck between the accuracy of the results and the simulation time. For this purpose, the time step is set to 156.25 μs, and the adaptive mesh refinement technique is applied, resulting in 140,728 mesh elements.

To investigate the influence of the RT, two sets of simulations are conducted. In the first analysis, the RT is removed, and the rotor winding is supplied directly with the input voltage source. In the second analysis, the RT is included in the simulation. The induced voltages in the signal windings are calculated and imported into MATLAB software. The synchronous sampling method is then employed to determine the envelope of the signals. Finally, by using the two desired envelopes, the position is calculated. The calculated position is compared with the actual position to determine the sensor's position error.

The Average of Absolute Position Error (AAPE) and the Total Harmonic Distortion (THD) of the output waveform envelopes are as key metrics for assessing the accuracy of synchros. These indices are used in the following section to compare the output results.

Table 1. Geometric dimensions and excitation parameters of the studied WR synchro.

Parameter	Unit	Value
Stator outer/inner diameter	mm	46/34
Rotor outer/inner diameter	mm	32/23.5
Synchro/ RT height	mm	6.7/5
Number of teeth for stator/rotor	-	12/20
Slot width of stator/rotor	mm	7.12/2.59
Slot height of stator/rotor	mm	2.6/2.41
Slot opening width of stator/rotor	mm	0.99/0.5
Number of turns for RT windings	-	50
Excitation voltage/frequency	V/Hz	5/400
Rotational speed	rpm	300

3.1 Simulation in the Ideal Condition

To extract signal voltages under ideal conditions (neglecting the effect of the RT), the rotor winding is directly supplied with a high-frequency excitation voltage. The output voltages of the synchro and their envelope, are shown in Fig. 2(a) and (b), respectively. The harmonic content analysis of the signal envelope, as illustrated in Fig. 2(c), shows that the maximum THD of the synchro's output voltage is 0.056%. In this case, the AAPE value has also been calculated to be 0.013°.

3.2 Simulation with Considering the Influence of RT's Leakage Flux

To account for the impact of the RT in TSFEA, the input voltage source is connected to the primary winding of the RT. With the RT's influence considered, the maximum THD of the output voltage envelope increases to 0.114%. This represents a sharp increase of 103.5% compared to the ideal condition, resulting in a higher position error for the sensor. The envelope of the induced voltages in the synchro's signal windings, both with and without the RT's effect, is shown in Fig. 3(a). From the waveforms in Fig. 3(a), not only is a phase shift observed between the corresponding envelopes of each phase, but the amplitude of the envelopes also decreases when the RT's effect is included. The position error of both sensors is presented in Fig. 3(b). The AAPE of the synchro, considering the RT, is 0.082°, which corresponds to a 530% increase compared to the case where the RT's effect was neglected.

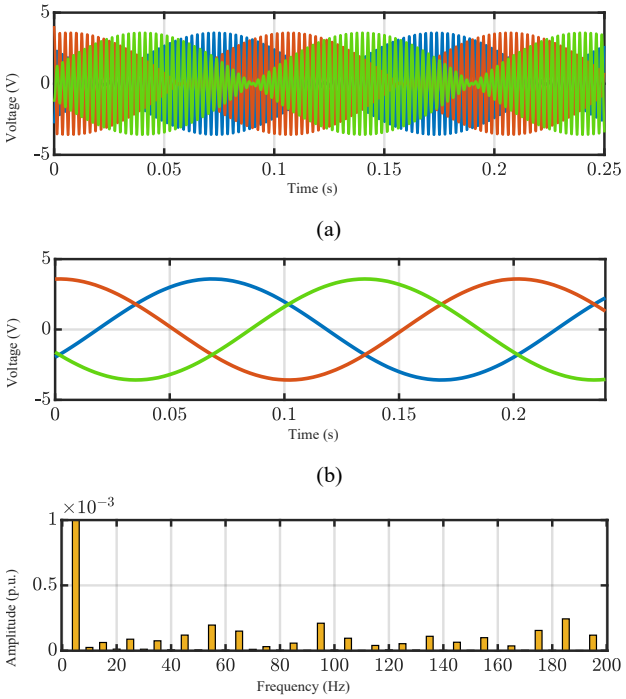

Fig 2. Finite element simulation results of the studied synchro, without considering the RT effect: (a) induced voltages in signal windings, (b) envelope of the induced voltages, and (c) harmonic content of the envelopes.

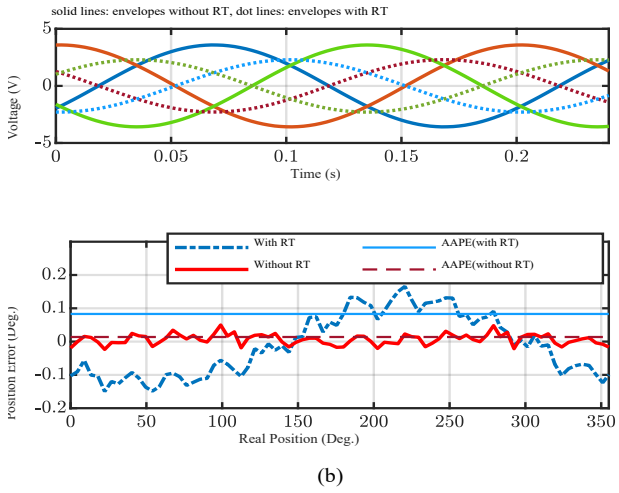

Fig 3. Finite element simulation results of the studied synchro: (a) comparison of the signal voltage envelopes and (b) position error analysis with and without considering the effect of the RT.

Therefore, the use of RT in WR synchros significantly impacts the precision of the sensor. To explain the reason, the flux paths in the RT, obtained from the 2-D finite element simulation, are presented in Fig. 4(a). For better clarity, the path of the RT's primary winding flux, which passes through the stator core, is shown in 3-D in Fig. 4(b).

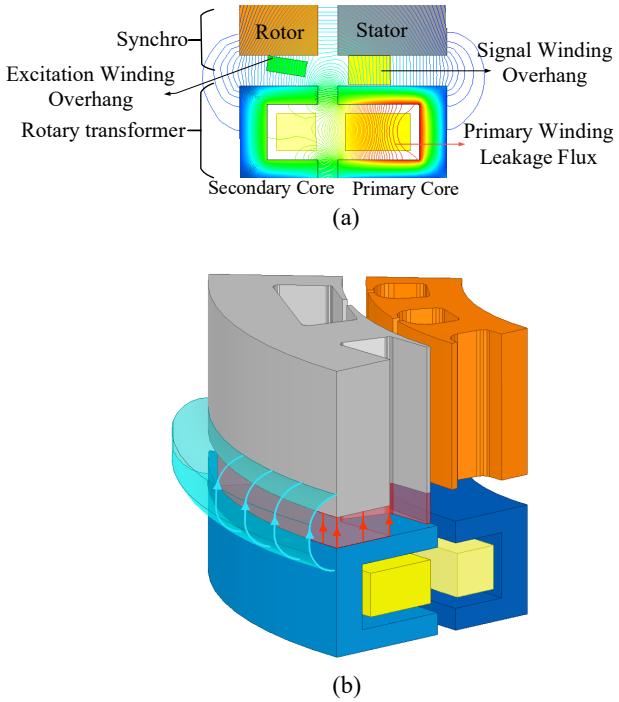

Fig 4. Determination of the RT's leakage flux paths and the flux through the synchro core using finite element analysis: (a) two-dimensional view, (b) and in three-dimensional view.

It is important to note that in Fig. 4, the dispersed fluxes in the surrounding space have been neglected. From Figs. 4(a) and (b), it can be observed that the leakage flux from the RT and the flux passing through the overhang of the signal windings contribute to an increase in the THD of the output signal, thereby reducing the sensor's accuracy.

The following presents methods for reducing the negative impact of the RT's leakage flux on the accuracy of WR synchros.

4 Design Improvement

Three different techniques are explored to minimize the impact of the RT's leakage flux on the accuracy of the synchro.

4.1 Increasing the Distance between the RT and Synchro Core

Increasing the distance (D) between the RT and the sensor is one method to reduce the impact of the RT's leakage flux. By doing so, the reluctance of the magnetic flux path between the signal windings' overhang and the

RT's core is increased. The distance, D, is defined as shown in Fig. 5, with its initial value set to 7.5 mm. In this configuration, the RT's leakage flux that surrounds the signal windings' overhang passes through the iron core of the transformer, which has lower reluctance. This effectively reduces the influence of the leakage flux on the output voltage.

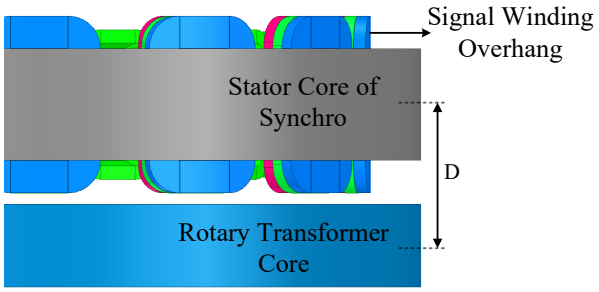

Fig 5. Definition of D as the distance between the synchro core and the RT core.

To determine the distance at which the impact of the transformer's leakage flux on the synchro's output voltages becomes negligible, the distance between the RT and the synchro is gradually increased. Using finite element analysis, the mutual inductance between the primary winding of the RT and one turn of the signal windings is calculated, as shown in Fig. 6. At a distance of 19.5 mm, the mutual inductance reduces to 46.27 nH. Further increasing the distance results in an excessive sensor length, which is undesirable. By calculating the envelope of the output voltages in this case, the maximum THD is reduced to 0.076%, representing a 33% decrease compared to the case where the RT's effect is considered. Additionally, the AAPE decreases by 72%, reaching 0.0247°.

Fig. 7 shows the output position error versus the actual position, at D=19.5 mm under ideal conditions, and D=7.5 mm for the studied synchro. As shown in Fig. 7, increasing D improves the sensor's accuracy, but at the cost of longer synchro length. Therefore, this approach may not be suitable for applications requiring small-sized sensors.

4.2 Introducing an Air Gap within the RT's Core

Another solution to increase the reluctance of the RT's flux path to the windings' overhang is to introduce an air gap in the core of the RT. Fig. 8 shows the proposed radial air gap with a length of 0.1 mm. Additionally, due to the direction of the magnetic flux in the RT core, the mutual inductance between the primary and secondary windings increases, thereby reducing the impact of the leakage flux on the synchro's output voltage. Based on the results from the 3-D TSFEA, the maximum THD of the output signal is 0.105%, which represents a 7.8% reduction compared to the scenario with the conventional RT. As shown in Fig. 9, which illustrates the synchro's position error relative to the actual position when accounting for the RT core gap, the AAPE decreases by 8.5%, reaching a value of 0.075°. To investigate the effect of slot width on the sensor's performance, the radial slot width is increased from 0.1 mm to 0.2 mm. In this case, the sensor's AAPE reaches 0.040°, and the THD of the signal envelope decreases to 0.103%, representing a reduction of 51.2% and 9.6%, respectively, compared to the synchro with a conventional RT. It can be concluded that increasing the radial slot width reduces the leakage flux linked with the signal winding overhang.

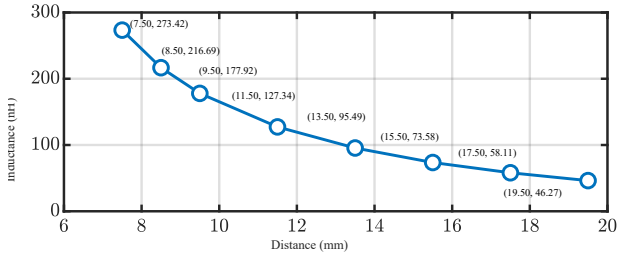

Fig 6. Mutual inductance between the RT's primary winding and the signal windings versus the distance between the RT and synchro.

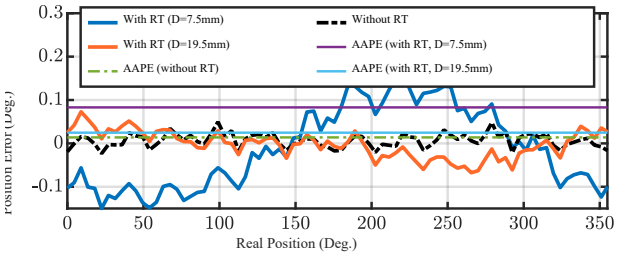

Fig 7. Comparison of position errors of the studied synchro with and without considering the effect of the RT, and with varying distances between the synchro and the RT core.

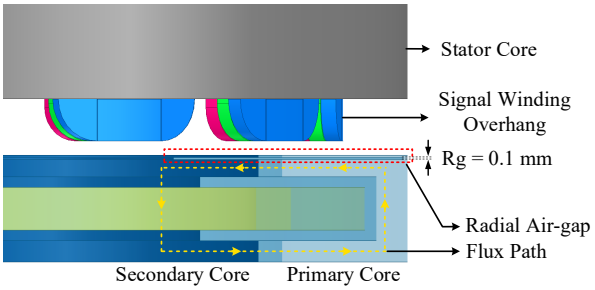

Fig 8. Implementation of an air gap in the RT core to mitigate the impact of leakage flux on the signal winding voltage.

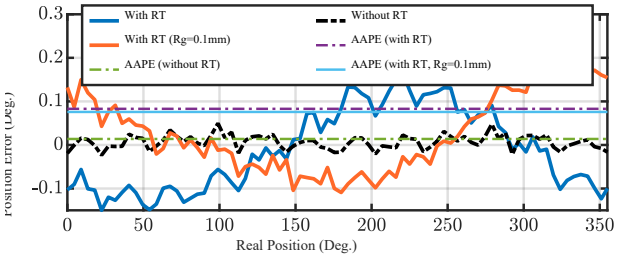

Fig 9. Examination of position errors for the studied synchro with and without considering the effect of the RT and the presence of an air gap (Rg) in the RT core.

In [32], the effect of different slot configurations on reducing leakage flux was not investigated. Therefore, in this study, a new type of slot is introduced in the RT

core, and its impact on sensor accuracy is evaluated. As shown in Fig. 4, a significant portion of the leakage flux coupled with the synchro is attributed to fringing flux. To reduce the fringing flux between the RT and synchro core, an axial slot with a width of 0.15 mm, as shown in Fig. 10, is introduced in both the primary and secondary cores of the RT. Fig. 11 presents the position error of the synchro for the RT with the axial slot. The AAPE of the sensor reaches 0.057°, representing a 30.4% reduction compared to the conventional RT structure. Additionally, the THD of the signal envelope decreases by 8.7%, reaching 0.104%. The results indicate that the slots introduced in the RT core effectively reduce leakage flux and improve the accuracy of the synchro.

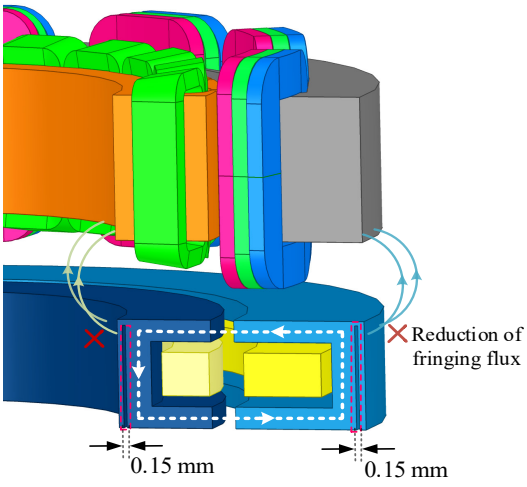

Fig 10. The axial gap created in the primary and secondary cores of the RT.

4.3 Electromagnetic Interference (EMI) shielding

In this section, a more effective method than those proposed in [32] is introduced. Electromagnetic Interference (EMI) shielding is employed as an alternative approach to mitigate the adverse effects of the RT's leakage flux on synchro accuracy. As shown in Fig. 12, an EMI shield attenuates electromagnetic waves through three mechanisms: absorption, reflection, and multiple reflections. The total EMI shielding effectiveness (SET) of a shielding material is the sum of the electromagnetic wave attenuation through absorption (SEA), reflection (SER), and multiple reflections (SEM), as expressed by Eq. (5) [33]:

$$SE_T = SE_R + SE_A + SE_M \tag{5}$$

The Absorption loss of the material can be calculated using Eq. (6) [33]:

$$SE_A = -8.68t\frac{\sqrt{f\mu_r\sigma_t}}{2} \tag{6}$$

where σ_T is the total electrical conductivity (in S/cm), f is the frequency, μ_r is the relative magnetic permeability, and t represents the thickness of the shielding material. According to Eq. (6), the shielding effectiveness due to the absorption mechanism improves with an increase in the electrical conductivity and magnetic permeability of the material. Therefore, iron (with μ_r=11000) is chosen for its high magnetic permeability, and copper is selected for its high electrical conductivity to reduce the RT's leakage flux. The sensor structure, integrated with the designed shield for the RT, is shown in Fig. 13. Based on the results from the 3-D TSFEA, as illustrated in Fig. 14, the copper shield outperforms the iron shield in mitigating the adverse effects of the RT's leakage flux. As shown in Fig. 14(a), the maximum THD of the signal envelope for the RT with the copper shield is 0.094%, representing a 17.5% reduction compared to the unshielded structure. Furthermore, as shown in Fig. 14(b), the AAPE has decreased by 63.3%, reaching 0.0304°, along with a reduction in the maximum position error of the sensor.

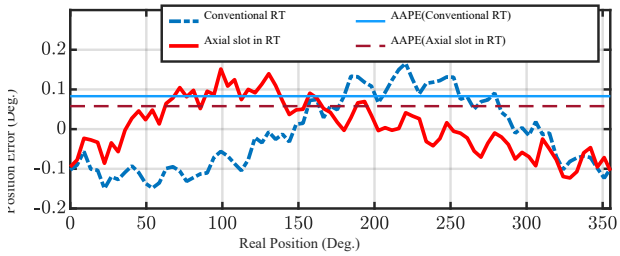

Fig 11. Comparison of the position error of the studied synchro with and without an axial slot in the current transformer core.

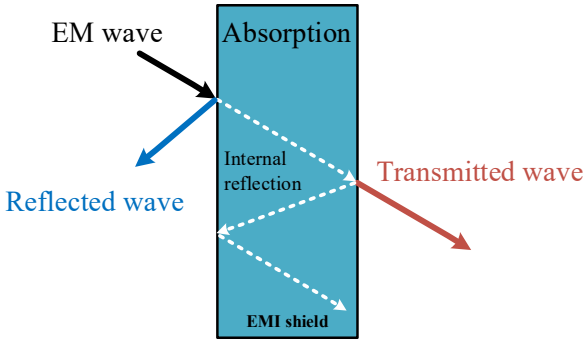

Fig 12. Different EMI Shielding Mechanisms.

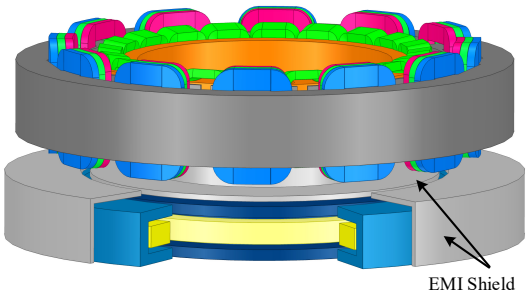

Fig 13. The studied synchro with shielded RT.

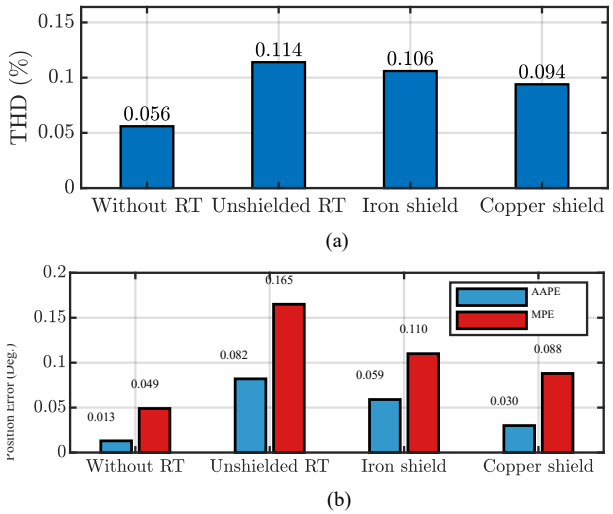

Fig 14. Comparing the performance of the studied synchro with different EMI materials: (a) THD of voltages' envelope (b) AAPE and MPE.

5 Experimental Evaluation

For the practical assessment of the proposed compensation methods, evaluations are conducted on a prototype sensor. Due to its effectiveness and ease of implementation, the first method is selected. Fig. 15(a) shows the stator and rotor core of the prototype, while Fig. 15(b) presents the built RT. The experimental test circuit of the prototyped synchro is illustrated in Fig. 15(c). As shown, a DC motor is used to rotate the sensor at a desired constant speed, and a precise optical encoder is coupled to the motor shaft as the reference position sensor. The primary winding of the RT is powered using a digitally synthesized function generator, and a digital oscilloscope is employed to measure and record the output voltages of the prototype synchro. These captured analog voltages are displayed in Fig. 16. The position error in the experimental test is calculated by comparing the determined position to the real position, where the real position is provided by the optical encoder. The obtained AAPE is 0.028°, which indicates that the deviation between the simulation and practical results is less than 11%, thus confirming the accuracy of the simulation.

6 Conclusion

In this study, the impact of the RT's leakage flux on the accuracy of WR synchros was analyzed using 3-D time-stepping finite element analysis (TSFEA). Three distinct methods for mitigating the negative effects of transformer leakage flux were proposed, and the results of both simulations and experiments were presented. In the first method, the influence of the RT's leakage flux was examined by increasing the distance between the synchro and the RT core, leading to the determination of an optimal distance where the effect of the leakage flux

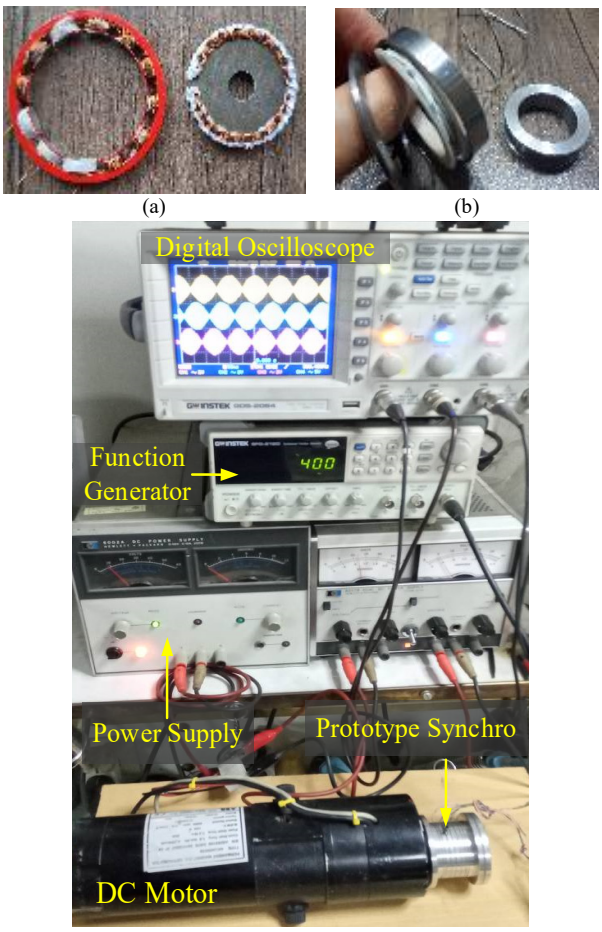

Fig 15. The prototype synchro: (a) the stator and rotor core, (b) the employed RT, and (c) the test circuit.

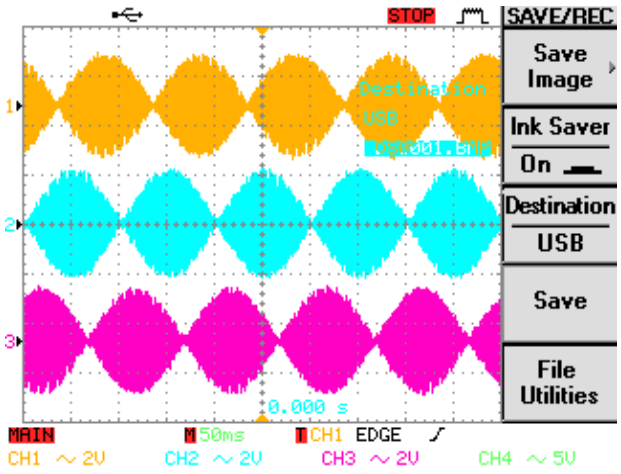

Fig 16. The measured voltages from the experimental test.

on synchro accuracy became negligible. In the second method, a gap was introduced within the RT's core to reduce the leakage flux passing through the signal windings' overhang. As an alternative approach, an

electromagnetic shielding frame was designed for the RT, and the performance of different shield materials was evaluated. The results showed that a copper-based electromagnetic shield significantly attenuates the negative impact of the RT's leakage flux, thereby improving the synchro's accuracy. Finally, a prototype of the investigated synchro was tested experimentally. The good agreement between the experimental data and the 3-D TSFEA results confirmed the accuracy of the simulations and validated the effectiveness of the proposed methods. Future research will focus on exploring additional shielding materials for the RT and their impact on synchro accuracy, analyzing various RT structures, and optimizing RT design to minimize leakage flux and further enhance the accuracy of WR synchros.

Conflict of Interest

The authors declare no conflict of interest.

Author Contributions

M.A. Razavi:

1) Idea & Conceptualization
2) Software and Simulation
3) Winding the prototype's cores

F. Tootoonchian:

1) Idea & Conceptualization
2) Supervision
3) Building the prototype and conducting experimental measurements

Z. Nasiri-Gheidari:

1) Idea & Conceptualization
2) Supervision
3) Revise & Editing

References

[1] W. Mi, J. Yu, Z. Cai, H. Zhao, F. Zhao and Y. Luo, "Feasibility Investigation on Sinusoidal-Reluctance Rotor Contour in Variable Reluctance Resolver," in IEEE Transactions on Magnetics, vol. 59, no. 11, pp. 1-5, Nov. 2023.

[2] X. Ge, Z. Q. Zhu, R. Ren and J. T. Chen, "A novel variable reluctance resolver for HEV/EV applications," 2015 IEEE International Electric Machines & Drives Conference (IEMDC), Coeur d'Alene, ID, USA, 2015, pp. 611-617.

[3] L. Sun, J. Taylor, X. Guo, M. Cheng and A. Emadi, "A Linear Position Measurement Scheme for Long-Distance and High-Speed Applications," in IEEE Transactions on Industrial Electronics, vol. 68, no. 5, pp. 4435-4447, May 2021.

[4] M. Bahari, F. Tootoonchian and A. Mahmoudi, "An Electromagnetic Design of Slotless Variable Reluctance PM-Resolver," in IEEE Transactions on Industrial Electronics, vol. 70, no. 5, pp. 5336-5346, May 2023.

[5] M. S. KhajueeZadeh, M. Emadaleslami, F. Tootoonchian, A. Daniar, M. C.Gardner and B. Akin, "Comprehensive Investigation of the Resolver' Eccentricity Effect on the Field-Oriented Control of PMSM,"in IEEE Sensors Journal, vol. 23, no. 17, pp. 19145-19152, 1 Sept.1, 2023.

[6] H. Saneie, Z. Nasiri-Gheidari and A. Belahcen, "On the Field-Reconstrution Method for Electromagnetic Modeling of Resolvers," in IEEE Transactions on Instrumentation and Measurement, vol. 72, pp. 1-8, 2023.

[7] P. Naderi and R. Ghandehari, "Comprehensive Analysis on a New Type VR-Resolver with Toroidal Windings Under Healthy and Eccentric Cases," in IEEE Transactions on Industrial Electronics, vol. 69, no. 12, pp. 13754-13762, Dec. 2022.

[8] Z. Qian, L. Qi, G. Li, W. Deng, Z. Sun and Q. Chen, "Analysis of Vibration and Noise in Electric Drive System Under Resolver and Motor Rotor Coupling Eccentricity," in IEEE Transactions on Transportation Electrification, vol. 10, no. 1, pp. 1827-1836, March 2024.

[9] S. A. Seyed-Bouzari, M. R. Eesazadeh, F. Tootoonchian and Z. Nasiri-Gheidari, "Development of a Multiturn Linear Variable Reluctance Resolver with Integrated Ferromagnetic Core," inIEEE Sensors Journal, vol. 24, no. 19, pp. 29898-29905, 1 Oct.1, 2024.

[10] M. R. Eesazadeh and Z. Nasiri-Gheidari, "Winding Selection for Wound-Rotor Synchro," in IEEE Sensors Journal, vol. 24, no. 1, pp. 215-222, 1 Jan.1, 2024.

[11] J. Zhou, Z. Song, X. Xiao, X. Huang and Y. Xie, "A Hybrid-Excited Resolver for High-Speed Operation," in IEEE Transactions on Power Electronics, vol. 39, no. 5, pp. 4958-4962, May 2024.

[12] P. Naderi, M. H. Rezaee and A. Ramezannezhad, "A Novel Robust Double-Side Linear Resolver Proposal with Toroidal Windings," in IEEE Transactions on Instrumentation and Measurement, vol. 73, pp. 1-8, 2024.

[13] P. Naderi, B. Ehsan-Maleki and A. Ramezannezhad, "A Robust High-Accuracy Wound Rotor Resolver Proposal with One and Two Pole Pairs," in IEEE

Sensors Journal, vol. 24, no. 7, pp. 9819-9827, 1 April1, 2024.

[14] S. Hajmohammadi and Z. Nasiri-Gheidari, "Proposal of a Wound-Rotor PCB-Resolver," in IEEE Transactions on Industrial Electronics, vol. 71, no. 11, pp. 15122-15129, Nov. 2024.

[15] F. Zare, F. Tootoonchian, A. Daniar, M. C. Gardner and B. Akin, "Magnetic Equivalent Circuit Model for Performance Prediction of Two-DOF Planar Resolver," in IEEE Access, vol. 11, pp. 102207-102216, 2023.

[16] X. Ran, J. Shang, M. Zhao and Z. Yi, "Improved Configuration Proposal for Axial Reluctance Resolver Using 3-D Magnetic Equivalent Circuit Model and Winding Function Approach," in IEEE Transactions on Transportation Electrification, vol. 9, no. 1, pp. 311-321, March 2023.

[17] M. R. Soleimani, Z. Nasiri-Gheidari, F. Tootoonchian and H. Oraee, "Optimal Design of Outer Rotor VR Resolver Based on MEC Model," in IEEE Sensors Journal, vol. 25, no. 3, pp. 4440-4447, 1 Feb.1, 2025.

[18] M. KhajueeZadeh, F. Zare and Z. Nasiri-Gheidari, "Reliability Analysis of Two Resolver Configurations Under Faulty Conditions in 2DOF System," in IEEE Transactions on Instrumentation and Measurement, vol. 72, pp. 1-8, 2023.

[19] P. Naderi, S. Sharouni and B. Ehsan-Maleki, "A Novel Robust Linear Resolver Proposal and Performance Analysis Under Healthy and Air-Gap Asymmetry Fault," in IEEE Transactions on Instrumentation and Measurement, vol. 72, pp. 1-8, 2023.

[20] H. Lasjerdi and Z. Nasiri-Gheidari, "Fault Detection in Variable Air-gap Resolver," 2023 14th Power Electronics, Drive Systems, and Technologies Conference (PEDSTC), Babol, Iran, Islamic Republic of, 2023, pp. 1-6.

[21] H. Lasjerdi and F. Tootoonchian, "Improving the Accuracy of Wound-Rotor Resolvers Under Inter-Turn Short Circuit Faults," in IEEE Sensors Journal, vol. 21, no. 5, pp. 5944-5951, 1 March1, 2021.

[22] M. Bahari and F. Tootoonchian, "Proposal of a Fault-Tolerance Technique for 1-ph Open Circuit Fault in Resolvers," in IEEE Sensors Journal, vol. 21, no. 14, pp. 15987-15992, 15 July15, 2021.

[23] A. Keyvannia and Z. Nasiri-Gheidari, "A Comprehensive Winding Method for Linear Variable-Reluctance Resolvers to Compensate for the End Effects," in IEEE Transactions on Industrial Electronics, vol. 70, no. 9, pp. 9593-9600, Sept. 2023.

[24] H. Saneie, Z. Nasiri-Gheidari, F. Tootoonchian and A. Daniar, "Simplified Winding Arrangement for Integrated Multiturn Resolvers," in IEEE Transactions on Industrial Electronics, vol. 68, no. 12, pp. 12802-12809, Dec. 2021.

[25] H. Saneie, Z. Nasiri-Gheidari, and F. Tootoonchian, “Design-oriented modelling of axial-flux variable-reluctance resolver based on magnetic equivalent circuits and Schwarz–Christoffel mapping,” IEEE Trans. Ind. Electron., vol. 65, no. 5, pp. 4322–4330, May 2018.

[26] Z. Nasiri-Gheidari, "Design, Analysis, and Prototyping of a New Wound-Rotor Axial Flux Brushless Resolver," in IEEE Transactions on Energy Conversion, vol. 32, no. 1, pp. 276-283, March 2017.

[27] S. Hajmohammadi and F. Tootoonchian, “Simplification of integrated multi-turn wound-rotor resolvers’ manufacturing,” IEEE Sensors J., vol. 20, no. 23, pp. 14141–14147, Dec. 2020.

[28] V. Abramenko, I. Petrov and J. Pyrhönen, "Variable Reluctance Resolver with a Modular Stator," 2023 IEEE International Electric Machines & Drives Conference (IEMDC), San Francisco, CA, USA, 2023, pp. 1-7.

[29] M. Ghafarzadeh, A. Kamali E., A. D. Aliabad, R. Abedini, and M. A. Tajeddini, “A new brushless synchro with look-up table error compensation,” Int. J. Numer. Model., Electron. Netw., Devices Fields, vol. 29, no. 4, pp. 577–591, Jul. 2016.

[30] M. R. Eesazadeh, Z. Nasiri-Gheidari and F. Tootoonchian, "Innovative Winding and Tooth-Pole Configurations in the Development of Variable Reluctance Synchro," in IEEE Sensors Journal, vol. 25, no. 2, pp. 2494-2501, 15 Jan.15, 2025.

[31] M.R. Eesazadeh, and Z. Nasiri Gheidari, “Proposal of Winding Arrangements for the WR Synchros to Facilitate the 3-phase to 2-phase Conversion without Scott-T Transformer,” Power Electronics and Drives: Systems and Technologies Conf. (PEDSTC), 2024.

[32] M. A. Razavi, F. Tootoonchian and Z. Nasiri-Gheidari, " Investigating the Impact of the Rotary Transformer’s Leakage Flux on the Accuracy of Brushless Synchros," 2024 4th International Conference on Electrical Machines and Drives (ICEMD), Tehran, Iran, Islamic Republic of, 2024, pp. 1-6.

[33] D. Wanasinghe and F. Aslani, "A review on recent advancement of electromagnetic interference shielding novel metallic materials and processes," Composites Part B: Engineering, vol. 176, p. 107207, 2019.

7 Biographies

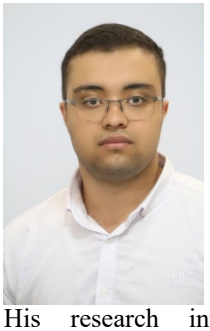

Mohammad Ali Razavi was born in Neyshabur, Iran, in 2000. He received the B.Sc. degree in Electrical Engineering from Shahid Rajaee Teacher Training University, Tehran, Iran, in 2023. Currently, he is pursuing the M.Sc. degree in Electrical Engineering at Sharif University of Technology, Tehran, Iran.
His research interests include the design and optimization of electromagnetic sensors.

Farid Tootoonchian received the B.Sc. and M.Sc. degrees in Electrical Engineering from the Iran University of Science and Technology, Tehran, Iran, in 2000 and 2007, respectively, and the Ph.D. degree from the K. N. Toosi University of Technology, Tehran, in 2012, all in electrical engineering. He is currently an Associate Professor in the Department of Electrical Engineering at Iran University of Science and Technology. His research interests include design, optimization, finite-element analysis, and prototyping of ultrahigh-speed electrical machines and ultrahigh-precision electromagnetic sensors.

Zahra Nasiri-Gheidari received the B.Sc. degree from the Iran University of Science and Technology, Tehran, Iran, in 2004, and the M.Sc. and Ph.D. degrees from University of Tehran, Tehran, in 2006 and 2012, respectively, all in electrical engineering. She is currently a Professor in the Department of Electrical Engineering at Sharif University of Technology. Her research focuses on the design, optimization, and performance analysis of electrical machines and electromagnetic sensors.